NJC
New Journal of Chemistry
A journal for new directions in chemistry

Accepted Manuscript

This article can be cited before page numbers have been issued, to do this please use: Y. Wu, A. Shi, H. Liu, Y. Li, W. Lun, H. Zeng and X. Fan, *New J. Chem.*, 2020, DOI: 10.1039/D0NJ03370G.

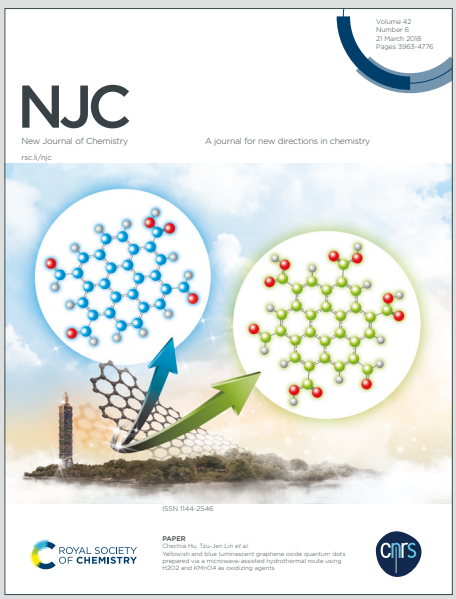

This is an Accepted Manuscript, which has been through the Royal Society of Chemistry peer review process and has been accepted for publication.

Accepted Manuscripts are published online shortly after acceptance, before technical editing, formatting and proof reading. Using this free service, authors can make their results available to the community, in citable form, before we publish the edited article. We will replace this Accepted Manuscript with the edited and formatted Advance Article as soon as it is available.

You can find more information about Accepted Manuscripts in the Information for Authors.

Please note that technical editing may introduce minor changes to the text and/or graphics, which may alter content. The journal's standard Terms & Conditions and the Ethical guidelines still apply. In no event shall the Royal Society of Chemistry be held responsible for any errors or omissions in this Accepted Manuscript or any consequences arising from the use of any information it contains.

View Article Online
DOI: 10.1039/D0NJ03370G

ARTICLE

A novel near-infrared xanthene-based fluorescent probe for detection of thiophenol *in vitro and in vivo*

Received 00th January 20xx,
Accepted 00th January 20xx

DOI: 10.1039/x0xx00000x

Yongquan Wu,[a,b] Aiping Shi,[a] Huiying Liu,[a] Yuanyan Li,[a] Weican Lun,[a] Hong Zeng*[a] and Xiaolin Fan*[a]

Thiophenol (or PhSH) is widely utilized for producing pesticides, dyes, and pharmaceuticals. However, high-concentration thiophenol not only has adverse effects on living organisms, but also causes environment pollution. Herein, we designed and synthesized a novel near-infrared (NIR) xanthene-based fluorescent probe (NOF) for real-time detection of thiophenol *in vitro* and *in vivo*. The probe NOF had good sensitivity and selectivity, and fast response towards thiophenol. The thiophenol-sensing mechanism was verified by high resolution mass spectra (HR-MS) and density functional theory (DFT) calculation. The probe NOF was also successfully applied to detect thiophenol in real water samples. Finally, owing to its NIR-emitting properties, it was successfully used for NIR fluorescent imaging of thiophenol in living cells and mice.

1. Introduction

Thiophenol (PhSH), also known as benzenethiol, belongs to a class of highly reactive and toxic aromatic thiols widely used for preparing pesticides, pharmaceuticals, and dyes.[1,2] Despite its usefulness, thiophenol is highly toxic, therefore is categorized as a class of pollutant compounds; it also has been listed as one of the prioritized pollutants.[3] Animal model studies have revealed that the median lethal dose in fish of thiophenol is 0.01–0.4 mM and that in mouse is 46.2 mg/kg.[4] Exposure to thiophenol can cause many symptoms, including vomit, nausea, muscular weakness, coughing, increased breathing, and even death, as it can cause damage to the central nervous system.[5-7] As a consequence, it is necessary to develop an easy, rapid, efficient method that can quantitatively detect thiophenol in the environment and in living organisms.

Fluorescence probing is one of the most prominent methods for detection of thiophenol due to its intrinsic advantages such as high sensitivity, good selectivity, technical simplicity, non-invasion, and in situ and real-time detection capability.[8-12] A number of fluorescent probes for the detection of thiophenol have been designed and developed to date.[13-34] Nevertheless, most of these fluorescent probes have slow response rates (longer than 10 min), relatively short emission wavelengths (in the visible region), and small Stokes shifts. The short emission wavelengths (λ_{max} < 650 nm) cause these fluorescent probes to have a shallow penetration depth, which is one of the causes that have limited their applications in imaging of deep tissues and the body. In addition, the body is a complex environment that can cause short-lived auto-fluorescence and tissue scattering, which can inevitably interfere with the imaging.[35-38] Therefore, the development of an NIR-emitting fluorescent probe that can sensitively and selectively detect and image thiophenol is highly desirable; however, such probes have rarely been reported in the literature.[39-41]

Xanthene fluorescent dyes have excellent photophysical properties, such as high fluorescence quantum yields, high tolerance to photobleaching, and high molar extinction coefficients, thus are good candidates for use as skeletons of fluorescent probes.[42-46] Herein, we present a novel NIR-emitting xanthene fluorescent probe (NOF) with a 'off-on' response mechanism that can sensitively and selectively detect thiophenol. The probe NOF was synthesized by attaching a strong electron-withdrawing 2,4-dinitrophenyl ether group to a xanthene skeleton, which served as an electron acceptor; the attachment caused the probe to emit weak fluorescence. But upon binding to thiophenol, the probe NOF exhibited a remarkably enhanced fluorescence signal. The probe NOF could effectively discriminate between thiophenol from aliphatic thiols and that from nucleophilic sulfides. It was also successfully applied to detect thiophenol in real water samples and to image thiophenol in living cells and in mice. The developed probe NOF can be applied to detect thiophenol in the environment or in other biological samples.

[a] *School of Chemistry and Chemical Engineering, Gannan Normal University, Shiyuan South Road, Ganzhou 341000, P. R. China, E-mail: fanxl@gnnu.edu.cn; zenghong@gnnu.edu.cn*
[b] *Jiangsu Key Laboratory for Biosensors, Institute of Advanced Materials (IAM), Nanjing University of Posts and Telecommunications, 9 Wenyuan Road, Nanjing 210023, P. R. China*
Electronic Supplementary Information (ESI) available. See DOI: 10.1039/x0xx00000x

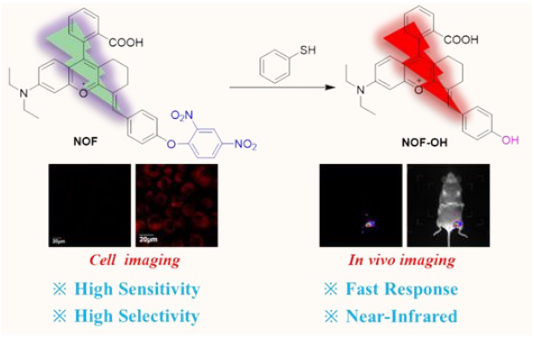

Scheme 1. Sensing mechanism of NOF in response to thiophenol (PhSH).

2. Experimental section

2.1 Materials

All commercial chemicals were purchased from commercial suppliers and used without further purification. 2-(4-diethylamino-2-hydroxybenzoyl) beozoic acid, acetic anhydride, cyclohexanone, and $HClO_4$ (70%) were purchased from Engery Chemical Technology Co., Ltd (China). Thiophenol, 3-aminothiophenol, 2,4-dinitrofluorobenzene, p-hydroxybenzaldehyde, and potassium acetate were purchased from Adamas Regent Co., Ltd (China). Potassium carbonate, potassium iodide, 4-hydroxybenzaldehyde was purchased from Aladdin Technology Co., Ltd (China). Concentrated H_2SO_4 was purchased from Jiangsu Tong Sheng Chemical Reagent Co., Ltd (China). Anhydrous DMF was purchased from J&K Scientific Ltd (China). Cysteine (Cys), and glutathione (GSH) were purchased from Aladdin Technology Co., Ltd (China). Homocysteine (Hcy) was purchased from Sigma-Aldrich Co., Ltd (China). MTT and PBS were purchased from Beyotime Biotechnology Co., Ltd (China). RPMI 1640 was purchased from Thermo Fisher Scientific Co., Ltd (USA).

2.2 Instruments

NMR spectra were obtained on a Bruker DRX-400 NMR spectrometer (Germany) with tetramethylsilane (TMS) as internal standard. High resolution mass spectra (HRMS) were obtained with an ESI ionization sources on Agilent 6540 Mass Spectrometer (USA). UV-Vis absorption spectra were recorded on a Shimadzu UV-2700 spectrophotometer (Japan). Emission spectra were recorded on an Edinburgh FS5 fluorescence spectrophotometer (UK). Cell imaging experiments were performed on an Olympus FV1000 laser scanning confocal microscopy (Japan). The absorbance values in MTT assay were measured using a Varioskan LUX microplate reader (Thermo Fisher Scientific Inc, USA). Mouse imaging experiments were carried out using an IVScpoe 7550 *in vivo* imaging system (Shanghai CLINX Science Instruments Ltd., China).

2.3 Synthesis section

The synthetic routes of compound 1, the probe NOF, and NOF-OH are shown in Scheme 2. Their structural characterization can be found in ESI.

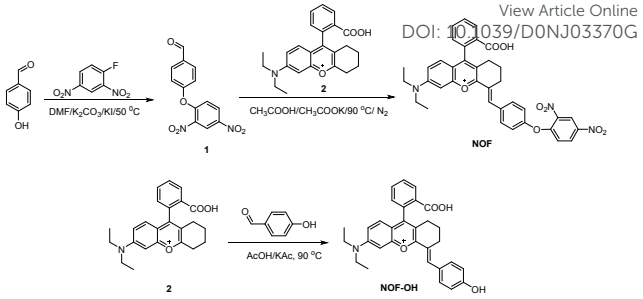

Scheme 2. Synthetic route of NOF and NOF-OH.

2.3.1 Synthesis of compound 1

p-Hydroxybenzaldehyde (305 mg, 2.5 mmol) was mixed with potassium carbonate (414 mg, 3 mmol) and N,N-dimethylformamide (3 mL) in a 50-mL three-necked flask. After that, 1-fluoro-2,4-dinitrobenzene (930 mg, 5 mmol) and potassium iodide (830 mg, 5 mmol) dissolved in N,N-dimethylformamide (3 mL) were added to the flask. The mixture was heated to 50 °C under N_2 atmosphere while being magnetically stirred for 5 h. After the reaction was completed, the reaction solution was suction filtered to remove the solid. The filtrate was transferred to a separatory funnel, into which an appropriate amount of deionized water and dichloromethane were added for extraction. The extraction was repeated three times, and the products in the organic layer were collected. Anhydrous sodium sulfate was added to the products to remove water for 2 h. The residue was subsequently evaporated to dryness under reduced pressure. The crude product was purified by silica gel column chromatography using CH_2Cl_2: petroleum ether (3:1) as an eluent, from which a white solid was obtained. ^{1}H NMR (400 MHz, $CDCl_3$) δ 10.00 (s, 1 H), 8.86 (d, *J* = 2.7 Hz, 1 H), 8.42 (dd, *J* = 9.2, 2.8 Hz, 1H), 8.02 – 7.95 (m, 2H), 7.28 (d, *J* = 2.1 Hz, 1H), 7.26 (d, *J* = 2.0 Hz, 1H), 7.23 (d, *J* = 9.1 Hz, 1H).

2.3.2 Synthesis of probe NOF

Compound 2 was synthesized according to a previously reported method and was used without further purification.[47]

Compound 1 (288 mg, 1 mmol), compound 2 (376 mg, 1 mmol), potassium acetate (98 mg, 1 mmol), and acetic anhydride (6 mL) were mixed in a 50-mL three-necked flask. The mixture was stirred at 90 °C for 5 h under N_2 atmosphere. After the reaction, an appropriate amount of water was added into the reaction mixture to remove excess acetic anhydride, and an appropriate amount of sodium hydrogen carbonate was slowly added thereafter. The precipitate was filtered under reduced pressure to obtain a solid crude product. The crude product was purified by silica gel column chromatography using CH_2Cl_2: ethyl acetate (3:5) as an eluent, from which a purple solid was obtained. ^{1}H NMR (400 MHz, CD_3OD) δ 8.88 (d, J = 2.8 Hz, 1H), 8.47 (dd, J = 9.2, 2.8 Hz, 1H), 8.11 (dd, J = 7.1, 2.0 Hz, 1H), 8.05 (s, 1H), 7.74 (d, J = 8.7 Hz, 2H), 7.68 – 7.59 (m, 2H), 7.30 (dd, J = 9.0, 4.0 Hz, 3H), 7.22 – 7.17 (m, 1H), 7.11 (d, J = 3.7 Hz, 3H), 3.67 (d, J = 7.1 Hz, 4H), 2.95 (d, J = 7.6 Hz, 2H), 2.53 – 2.30 (m, 2H), 1.81 (d, J = 8.5 Hz, 2H), 1.29 (d, J = 7.1 Hz, 6H). HR-MS (ESI), chemical formula: $C_{37}H_{32}N_3O_8^+$, calcd, 646.2184; found: 646.2186.

View Article Online
DOI: 10.1039/D0NJ03375C

2.3.3 Synthesis of NOF-OH

p-Hydroxybenzaldehyde (0.10 g, 0.82 mmol) was reacted with compound 2 (0.34 g, 0.90 mmol) in 15 mL acetic acid overnight. The crude product was then purified by silica gel column chromatography to obtain a dark purple solid (0.10 g, yield = 24%). ^{1}H NMR (400 MHz, Methanol-d_4) δ 8.14 (q, J = 4.2, 3.3 Hz, 1H), 8.08 (d, J = 16.4 Hz, 1H), 7.71 – 7.60 (m, 2H), 7.56 (q, J = 8.2 Hz, 2H), 7.22 – 7.09 (m, 4H), 6.91 (q, J = 7.6, 6.6 Hz, 2H), 3.76 – 3.58 (m, 4H), 2.94 (s, 2H), 2.59 – 2.35 (m, 2H), 1.83 (s, 2H), 1.34 – 1.29 (m, 6H). HR-MS (ESI), chemical formula: $C_{31}H_{30}NO_4^+$ [M+H]$^+$: calcd, 480.2169; found: 480.2346..

2.4 Measurement of UV–vis absorption and fluorescence spectra

The UV–vis absorption and fluorescence spectra of thiophenol was carried out in DMSO/PBS solution (v/v, 1:1, pH=7.4) by which a certain amount of thiophenol standard solution (2 mM) was added dropwise to the solution of the probe NOF. The mixture was stirred for 10 min before being subjected to the test. The UV-vis absorption spectra were collected at a wavelength range of 400 to 800 nm. The fluorescence spectra were collected at an excitation wavelength of 670 nm and an emission wavelength range of 690 to 850 nm.

2.5 Determination of selectivity towards thiophenol

The UV-visible absorption and fluorescence spectra of the probe NOF (10 μM) were measured in DMSO/PBS (v/v, 1:1, pH=7.4) in the presence of various analytes, including dithiothreitol (DTT), GSH, Hcy, Cys, Phe, Trp, Leu, $ONOO^-$, $S_2O_8^{2-}$, NO^{3-}, NO^{2-}, S^{2-}, ClO^-, SCN^-, Na^+, K^+, Ca^{2+}, Cd^{2+}, Cu^{2+}, Ni^{2+}, Pb^{2+}, CO^{2+}, Zn^{2+}, Mg^{2+}, and Cr^{3+}, as well as of thiophenol. Before the measurement, the probe solution was incubated at 37 °C for 10 min.

2.6 Detection of thiophenol in real water samples by the probe NOF

The detection of thiophenol in real water samples (including tap water and mineral water from NongFu Spring) by the probe NOF was carried out in PBS buffer (10 mM, pH = 7.4) containing 1 mM CTAB at 37 °C. The water samples were spiked with thiophenol at various final concentrations (0, 5, 10, and 15 μM) prior to being added with the probe NOF (final concentration = 10 μM). The fluorescence spectra of the samples were then measured at 740 nm. The experiments were carried out in triplicate, and the data were reported as mean ± standard deviation.

2.7 Computational details

To further understand the optical properties of the NOF and NOF-OH, we optimized the molecular structure of the ground and excited states of the NOF and NOF-OH at the B3LYP/6-31G (d) level using density functional theory (DFT).[48,49] Time-dependent DFT (TD-DFT) calculations were performed to get the nature of the excited states based on the optimized structures.[50] All calculations were performed using Gaussian 09 Rev. D.01.[51]

2.8 Cell culture and cytotoxicity assay

To MCF-7 cells, which were provided by the Institute of Biochemistry and Cell Biology (Chinese Academy of Sciences), were used as the model cells and were cultured in RPMI 1640 medium supplemented with 10% (v/v) fetal bovine serum. The cells used for cell imaging were cultured on a confocal imaging dish overnight at 37 °C under 5% CO2 atmosphere for 24 h.

In vitro cytotoxicity of the probe was determined using MTT assay and MCF-7 cells grown to the logarithmic phase in a 96-well flat-bottomed microplate (cell density = 1 × 10^4 cells per well). Cell viability was determined as the amount of the formazan product formed in each well measured by OD490 in relative to OD690. Cell viability was calculated using the following formula: cell viability (%) = (average of (OD490 - OD690) of sample/average of (OD490 - OD690) of blank) × 100%. The data were expressed as mean of 4 parallel experiments ± standard deviation.

2.9 Cell imaging

In the control group, the cells were incubated with the probe NOF (10 μM) in a medium containing 0.5%(v/v) dimethyl sulfoxide at 37 °C for 30 min. In the experimental group, the cells were pretreated with various concentrations of thiophenol in DMSO for 2 h. After that, they were washed three times with PBS to remove excess thiophenol before being treated with the probe NOF (10 μM) for 30 min. All treated cells were subjected to fluorescence imaging using a confocal fluorescence microscope (Olympus FV1000, Japan).

2.10 Luminescence imaging in mice

All animal experiments were carried out in accordance with the guidelines of the Animal Protection and Use Committee of the Gannan Normal University and approved by the Animal Ethics Committee of the Department of Science and Technology of Jiangxi Province. Prior to the injection, Kunming mice were anesthetized with a certain amount of chloral hydrate (10% wt) and were then carefully placed in the animal imaging system. One side of the groin of the mice was injected with the probe NOF (20 μM, 50 μL), whereas the other side was first injected with thiophenol (50 μM, 50 μL) before being injected with the probe NOF (20 μM, 50 μL). The change of the fluorescence intensity in the mice was observed after a certain period of time. The fluorescence imaging was performed on an IVScope 7550 imaging system (Shanghai CLINX Science Instruments Ltd., China) using a long pass filter to collect fluorescence signals greater than 650 nm under excitation at 635 nm. The fluorescence imaging images were analyzed using ImageJ software.

3. Results and discussion

3.1 Design and synthesis of probe NOF

According to the literature, nitro-substituted phenyl ether can serve as a potential reaction site for thiophenols. Therefore, in this work, 2,4-dinitrophenyl moiety was used as an effective thiophenol-sensing group to modify xanthene skeleton to synthesize the probe NOF. Due to the fluorescence quenching effect of the nitro group, the fluorescence of this molecular system should be quenched by the 2,4-dinitrophenyl moiety. However, upon interaction with thiophenol, the 2,4-

dinitrophenyl moiety can be uncaged, in turn causing the fluorescent to be turned on (turn-on signal).

Firstly, 4-hydroxybenzaldehyde and 1-fluoro-2,4-dinitrobenzene were used as the raw materials to synthesize compound 1 under basic conditions. The compound 1 was then used to react with xanthene precursor 2 through Knoevenagel method to form the target probe NOF (Scheme 2). NOF-OH, which was used as a control fluorescent molecule, was also synthesized from 4-hydroxybenzaldehyde and xanthene precursor 2 via a one-step synthesis method. The structures of the probe NOF and NOF-OH were characterized by nuclear magnetic resonance spectroscopy (NMR) and high-resolution mass spectrometry (HR-MS) (Details can be found in the synthesis section and SI).

3.2 Photophysical properties of the probe NOF in the presence of thiophenol

The UV-vis absorption and fluorescence spectra of NOF in the presence of thiophenol at different concentrations (0 – 30 μM) were first determined in PBS: DMSO (1:1, v/v) at 37 °C for 10 min. Initially, we examined the absorption spectra of NOF upon continuous addition of thiophenols, from which we found that continuous addition of thiophenols (0–3.0 equiv.) into buffer caused the absorption peak to become gradually red-shifted to 675 nm. This is likely due to that the 2,4-dinitrophenyl moiety in NOF was transformed into a phenol group to generate NOF-OH (Scheme 1). The fluorescence response of NOF to thiophenol was subsequently examined. As can be seen in Fig. 1b, free NOF exhibited a relatively weak fluorescence signal after being excited at 670 nm. Upon the addition of thiophenol, the fluorescence signal at 740 nm was increased by up to 10 folds. Furthermore, the fluorescence titration assay revealed that the increase of the fluorescence intensity was in a dose-dependent manner; the fluorescence reached saturation when 30 μM thiophenol was added (Fig. 1b). A good linear relationship (R^2 = 0.996) between the fluorescence intensity at 740 nm and the concentration of thiophenol (2–18 μM) was also observed (Fig. S1). The thiophenol-detection limit of NOF (calculated by 3σ/k) was found to be as low as 0.120 μM, indicating that the probe NOF can detect trace amounts of thiophenol.

The fluorescence intensity of NOF (10 μM) as a function of time in the presence of thiophenol (1.5 and 2.5 equivalents) is displayed in Fig. 2. The fluorescence intensity was drastically enhanced within a few minutes after thiophenol was added, and reached a plateau after 10 min. Such fluorescence response suggests that the probe is suitable for real-time detection of thiophenol.

In order to extend further applicability of probe NOF under biological conditions, fluorescence intensity changes of NOF in aqueous solution were investigated at different pH values in presence or absence of thiophenol. As shown in Fig. S2, this probe can detect PhSH effectively under physiological pH condition (PH=7.4). Secondly, to determine whether NOF was photostable under excitation for a long time, its photostability in solution was assessed. The fluorescence intensity of was maintained over 95% of its initial value when monitored over a period of 60 min under excitation at 670 nm (Fig S3). This observation indicated that NOF is responsible for sensing with no obvious photobleaching.

Compared with other reported probes (Table S1), this probe has advantages for thiophenol detection including relatively low detection limit and more red-shift excitation and emission wavelengths. As a result, this probe can be used for *in vivo* imaging by excited at longer wavelength.

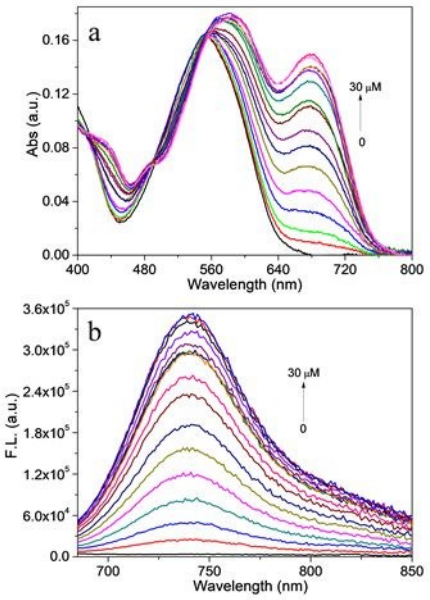

Fig. 1 Changes in emission spectra of NOF (10 μM) upon addition of increasing concentrations of PhSH (0 – 30 μM), PBS:DMSO=1:1 (v/v, pH=7.4). λ_{ex} = 670 nm.

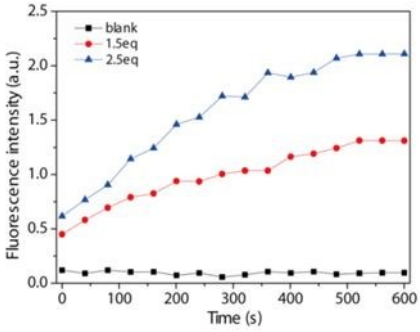

Fig. 2 Changes of fluorescence intensity at 740 nm of NOF (10 μM) + PhSH (15 and 25 μM) with different time. λ_{ex} = 670 nm, λ_{em} = 740 nm.

3.3 Selectivity towards thiophenol

To examine the selectivity of the probe NOF towards thiophenol, we measured the fluorescence response of the probe NOF (10 μM) in the presence of various analytes (5.0 equivalents each), including small molecules (Cys, Hcy, GSH, Trp, Leu, Phe, DTT) and anions (NO_3^-, NO_2^-, $ONOO^-$, $S_2O_8^{2-}$, S^{2-}, ClO^-, SCN^-) and compared them with the response in the presence of thiophenol. As shown in Fig. 3 and Fig. S4, only the presence of thiophenol caused significant fluorescence

View Article Online
DOI: 10.1039/D0NJ03370C

enhancement, whereas the presence of other analytes only caused slight change of fluorescence. The significant increase of fluorescence of the probe NOF was not observed in the presence of active sulfur-containing compounds (Cys, HCy, and S2-) other than thiophenol may be due to the local soft and hard acid-base principle. The local softness of the sulfur atom in these nucleophiles are different, thus respond differently at different strengths to the probe NOF. Moreover, the selectivity of NOF for PhSH over metal ions was also evaluated. As shown in Fig S5, the coexistent metal cations had a negligible interfering effect on the fluorescence intensity of NOF upon addition of PhSH. These data suggest that the probe NOF has high selectivity towards thiophenol.

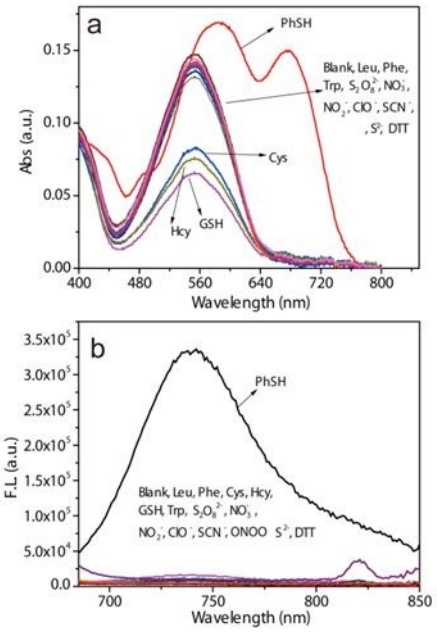

Fig. 3 (a) Absorption spectra and (b) fluorescence spectra of probe NOF (10 μM) treated with various analytes (DTT, GSH, Hcy, Cys, Phe, Trp, Leu, $ONOO^-$, $S_2O_8^{2-}$, NO_3^-, NO_2^-, S^{2-}, ClO^-, SCN^-, and PhSH), λ_{ex} = 670 nm, $\lambda_{em\ max}$= 740 nm.

3.4 Thiophenol-sensing mechanism

To investigate the mechanism of the probe NOF in sensing thiophenol, we first carried out a reaction between the probe NOF (10 μM) and thiophenol (PhSH) and then separated the reaction product (NOF+PhSH) by silica gel chromatography. We subsequently measured the UV-vis absorption and fluorescence spectra of the product NOF+PhSH and compared them with those of NOF-OH, from which we observed that the UV-vis absorption and fluorescence spectra of NOF-OH were similar to those of NOF+PhSH (Fig. S6). We also examined the change of the molecular weight of the probe NOF before and after reacting with thiophenol by high-resolution mass spectrometry (HR-MS). As shown in Fig. 4a, the peak of the probe NOF appeared at m/z = 646.2186 (calculated M^+ 646.2184). As shown in Fig. 4b, after reacting with thiophenol, a new peak corresponding to the molecular weight of NOF-OH appeared at m/z = 480.2165 (calculated M^+ 480.2169). These results demonstrate that the probe NOF senses thiophenol by first reacting with it and then generating NOF-OH.

To gain insights into the electronic properties and the 'off–on' fluorescence response of the probe NOF in the presence of thiophenol, we employed calculated DFT/TD-DFT data for both NOF and NOF-OH using B3LYP method on the basis of 6-31G (d). The energies for the frontier MOs as well as their corresponding highest occupied molecular orbital (HOMO) and lowest unoccupied molecular orbital (LUMO) gaps are listed in Table S2 (ESI†), and the HOMO-LUMO diagram is shown in Fig. 5 (More details can also be found in Fig. S7, ESI†). According to the data, the HOMO of NOF was located in the fluorophore, while its LUMO and LUMO+1 were located in the whole molecule and the 2,4-dinitrobenyl group, respectively. The lowest-energy transition of NOF was mainly the result of the orbital transitions from HOMO to LUMO and HOMO to LUMO+1. The latter orbital transition indicates that an electron was transferred from the excited state of fluorophore to the LUMO of the electron acceptor 2,4-dinitrobenyl moiety, which in turn caused the fluorescence quenching of NOF.

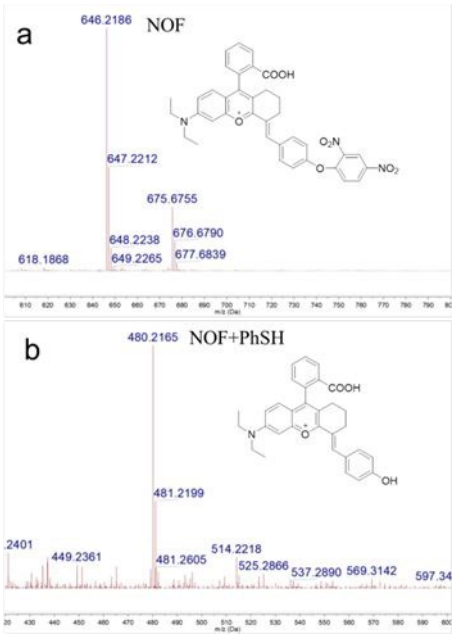

Fig. 4 HR-MS of (a) NOF and (b) product of NOF+PhSH.

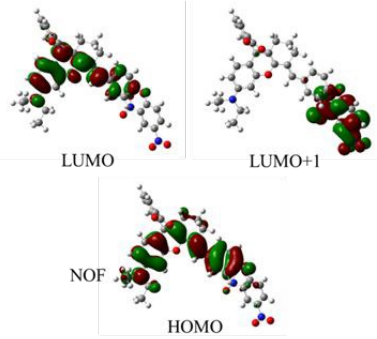

Fig. 5 Representations of the frontier molecular orbitals (MOs) for the S_0 geometry of NOF as determined at the DFT//B3LYP/6-31G* level.

3.5 Analysis of thiophenol in real samples by the probe NOF

The ability of the probe NOF to detect thiophenol in real water samples, including tap water and mineral water, was investigated. All water samples' pH value was adjusted to 7.4 using PBS buffer (10 mM) containing 1 mM CTAB. The water samples were spiked with different concentrations of thiophenol (0, 5, 10, and 15 μM) before adding the probe NOF; after that, the fluorescence intensity of NOF in the water samples was measured. As shown in Table 1, the recovery of thiophenol in tap water and mineral water were good with values ranging from 91.0% to 101.0%. These results indicate that the probe NOF can be used as a reliable tool for analysis of thiophenol in real water samples.

Table 1. Determination of thiophenol concentrations in real water samples.

Sample	Thiophenol spiked (μM)	Thiophenol recovered (μM)	Recovery (%)
Tap water	0.0	Not detected	—
	5.0	4.61±0.37	92.2
	10.0	9.95±0.23	99.5
	15.0	14.72±0.32	98.1
Mineral water	0.0	Not detected	—
	5.0	4.55±0.42	91.0
	10.0	10.10±0.33	101.0
	15.0	15.12±0.21	100.8

3.6 Cytotoxicity and imaging of thiophenol in cells

We first determined the cytotoxicity of the probe NOF by MTT assay. The results showed that viability of cells incubated with the probe NOF at various concentrations (5-20 μM) for 24 h was high (> 90% cell viability at 10 μM; Fig. S8, ESI†), indicating that the probe NOF has low cytotoxicity. This finding indicates that the probe NOF is biocompatible, thus is suitable for bio-imaging.

We then examined the ability of the probe NOF to detect thiophenols in living cells (MCF-7 cells) by laser confocal fluorescence microscopy. As illustrated in Fig. 6, the cells incubated with thiophenol (50 μM) and the probe NOF (10 μM) exhibited a significant fluorescence enhancement. By contrast, the cells incubated only with the probe NOF exhibited a weak fluorescent signal. This result indicates that the probe NOF can detect intracellular thiophenol.

3.7 *NIR imaging of PhSH in living animal*

In addition to its biocompatibility and high selectivity towards thiophenol, another unique characteristic of the probe NOF is its emission wavelength in the NIR region. Therefore, we carried out NIR imaging of thiophenol using the probe NOF in living animals, using mice as an animal model. Mice were subcutaneously injected with the probe NOF, followed by thiophenol. Thiophenol was injected into the right groin of mice in the experimental group (red circle), but saline was injected into the left groin of mice in the control group (green circle). Fluorescence images of mice (Fig. 7) showed that the fluorescence signal of mice in the experimental group was significantly higher than that of mice in the control group. This indicates that the probe NOF can detect thiophenol in real time and *in vivo*, thus may be used to further investigate the toxicological effects of thiophenol. Nonetheless, these are only the preliminary results showing the applicability of the probe NOF; the detection of thiophenol by the probe NOF in other animals or tissues should be further carried out in future studies.

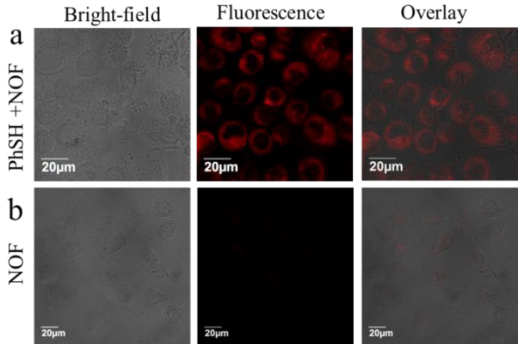

Fig. 6 Confocal luminescence images of living MCF-7 cells. MCF-7 cells were incubated with (a) PhSH (50 μM) for 1 h and then incubated NOF (5 μM); (b) MCF-7 cells were incubated NOF (5 μM). Emission was collected by a NIR channel at 650−750 nm, under excitation with 543 nm laser, scale bar = 20 μm.

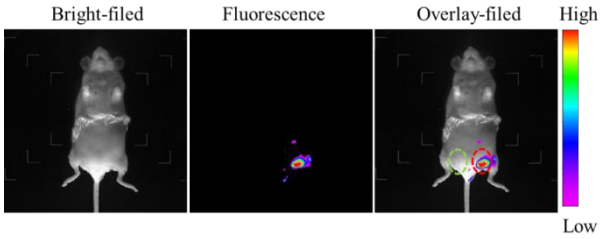

Fig. 7 NIR luminescence images of living mice. Mouse was subcutaneously injected in abdomen with 50 μL normal saline + NOF (20 μM, 50 μL) (green circle, left groin) and PhSH (50 μL, 50 μM) + NOF (20 μM, 50 μL) (red circle, right groin), the images was captured after 20 min. Emissions were collected at > 650 nm as detection signals, upon irradiation at 635 nm laser.

4. Conclusions

In summary, we successfully designed and synthesized an 'off-on' NIR fluorescent probe (NOF) for detection of thiophenol *in vitro* and *in vivo*. The probe had various remarkable advantages including high sensitivity, high selectivity and fast response towards thiophenol. It could recover thiophenol in real water samples with high recovery rates of 91.0%–101.0%. In addition, the probe NOF had low toxicity and good cell permeability, thus was successfully employed to image intracellular thiophenol. Finally, the probe was successfully applied in the fluorescence imaging of thiophenol in living mice. In future studies, the developed probe NOF ought to be applied to detect and image thiophenols in other environmental and biological samples.

Conflicts of interest

There are no conflicts to declare.

View Article Online
DOI: 10.1039/D0NJ03370G

Acknowledgements

This work was financially supported by the National Natural Science Foundation of China (21967001), the Natural Science Foundation of Jiangxi Province (20192BAB213004), the open research fund of Jiangsu Key Laboratory for Biosensors (JKLB201909), and the Training Plan for Innovation and Enterprise of Gannan Normal University (201910418004).

Notes and references

1 I. C. Popoff, J. R. Frank, C. B. Thanawalla and R. A. Creager, *J. Agric. Food Chem.*, 1972, **20**, 80-82.
2 A. Eychmüller and L. Rogach Andrey, *Pure App. Chem.*, 2000, **72**, 179.
3 K. Shimada and K. Mitamura, *J. Chromatogr. B*, 1994, **659**, 227-241.
4 T. P. Hell and R. C. Lindsay, *J. Environ. Sci. Health B*, 1989, **24**, 349-360.
5 T. R. Juneja, R. L. Gupta and S. Samanta, *Toxicol. Lett.*, 1984, **21**, 185-189.
6 R. Munday, *J. Appl. Toxicol.*, 1985, **5**, 402-408.
7 P. Amrolia, S. G. Sullivan, A. Stern and R. Munday, *J. Appl. Toxicol.*, 1989, **9**, 113-118.
8 X. Chen, Y. Zhou, X. Peng and J. Yoon, *Chem. Soc. Rev.*, 2010, **39**, 2120-2135.
9 Y. Yang, Q. Zhao, W. Feng and F. Li, *Chem. Rev.*, 2013, **113**, 192-270.
10 X. Zhang, J. Yin and J. Yoon, *Chem. Rev.*, 2014, **114**, 4918-4959.
11 (a) H. Zhu, J. Fan, J. Du and X. Peng, *Acc. Chem. Res.*, 2016, **49**, 2115-2126.(b) X.-P. He, X.-L. Hu, T. D. James, J. Yoon and H. Tian, *Chem. Soc. Rev.*, 2017, **46**, 6687-6696.
12 (a) J. Gao, Y. Tao, J. Zhang, N. Wang, X. Ji, J. He, Y. Si and W. Zhao, *Chem.-Eur. J.*, 2019, **25**, 11246-11256. (b) N. Wang, M. Chen, J. Gao, X. Ji, J. He, J. Zhang and W. Zhao, *Talanta*, 2019, **195**, 281-289. (c) J. Zhang, N. Wang, X. Ji, Y. Tao, J. Wang and W. Zhao, *Chem.-Eur. J.*, 2020, **26**, 4172-4192.
13 W. Jiang, Q. Fu, H. Fan, J. Ho and W. Wang, *Angew. Chem. Int. Ed.*, 2007, **46**, 8445-8448.
14 W. Jiang, Y. Cao, Y. Liu and W. Wang, *Chem. Commun.*, 2010, **46**, 1944-1946.
15 W. Lin, L. Long and W. Tan, *Chem. Commun.*, 2010, **46**, 1503-1505.
16 Z. Wang, D.-M. Han, W.-P. Jia, Q.-Z. Zhou and W.-P. Deng, *Anal. Chem.*, 2012, **84**, 4915-4920.
17 J. Li, C.-F. Zhang, S.-H. Yang, W.-C. Yang and G.-F. Yang, *Anal. Chem.*, 2014, **86**, 3037-3042.
18 D. Yu, F. Huang, S. Ding and G. Feng, *Anal. Chem.*, 2014, **86**, 8835-8841.
19 X. Shao, R. Kang, Y. Zhang, Z. Huang, F. Peng, J. Zhang, Y. Wang, F. Pan, W. Zhang and W. Zhao, *Anal. Chem.*, 2015, **87**, 399-405.
20 W. Zhang, X. Liu, H. Zhang, C. Feng, C. Liu, M. Yu, L. Wei and Z. Li, *J. Mater. Chem. C*, 2015, **3**, 8248-8254.
21 X. Liu, F. Qi, Y. Su, W. Chen, L. Yang and X. Song, *J. Mater. Chem. C*, 2016, **4**, 4320-4326.
22 Y. Yue, F. Huo, Y. Zhang, J. Chao, R. Martínez-Máñez and C. Yin, *Anal. Chem.*, 2016, **88**, 10499-10503.
23 W. Chen, X. Yue, W. Li, Y. Hao, L. Zhang, L. Zhu, J. Sheng and X. Song, *Sens. Actuators B Chem.*, 2017, **245**, 702-710.
24 X.-L. Liu, L.-Y. Niu, Y.-Z. Chen, Y. Yang and Q.-Z. Yang, *Sens. Actuators B Chem.*, 2017, **252**, 470-476.
25 H. Shang, H. Chen, Y. Tang, Y. Ma and W. Lin, *Biosens. Bioelectron.*, 2017, **95**, 81-86.
26 X. Xie, M. Li, F. Tang, Y. Li, L. Zhang, X. Jiao, X. Wang and B. Tang, *Anal. Chem.*, 2017, **89**, 3015-3020.
27 L. Xiong, J. Ma, Y. Huang, Z. Wang and Z. Lu, *ACS Sens.*, 2017, **2**, 599-605.
28 Y. Geng, H. Tian, L. Yang, X. Liu and X. Song, *Sens. Actuators B Chem.*, 2018, **273**, 1670-1675.
29 F. Wu, H. Wang, J. Xu, H.-Q. Yuan, L. Zeng and G.-M. Bao, *Sens. Actuators B Chem.*, 2018, **254**, 21-29.
30 S. Zhou, Y. Rong, H. Wang, X. Liu, L. Wei and X. Song, *Sens. Actuators B Chem.*, 2018, **276**, 136-141.
31 Y. Li, W. Su, Z. Zhou, Z. Huang, C. Wu, P. Yin, H. Li and Y. Zhang, *Talanta*, 2019, **199**, 355-360.
32 Q. Liu, A. Li, X. Li, B. Li, Y. Zhang, J. Li and Y. Guo, *Sens. Actuators B Chem.*, 2019, **283**, 820-830.
33 T. Xu, S. Zhao, X. Wu, L. Zeng and M. Lan, *ACS Sustain. Chem. Eng*, 2020, **8**, 6413-6421.
34 L. Yang, Y. Li, H. Song, H. Zhang, N. Yang, Q. Peng, L. Ji and G. He, *Dyes Pigments*, 2020, **175**, 108154.
35 R. Weissleder, *Nat. Biotechnol.*, 2001, **19**, 316-317.
36 L. Yuan, W. Lin, S. Zhao, W. Gao, B. Chen, L. He and S. Zhu, *J. Am. Chem. Soc.*, 2012, **134**, 13510-13523.
37 F. Kong, Z. Liang, D. Luan, X. Liu, K. Xu and B. Tang, *Anal. Chem.*, 2016, **88**, 6450-6456.
38 Y. Fang, W. Chen, W. Shi, H. Li, M. Xian and H. Ma, *Chem. Commun.*, 2017, **53**, 8759-8762.
39 Y. Pan, T.-B. Ren, D. Cheng, Z.-B. Zeng, L. Yuan and X.-B. Zhang, *Chem.–Asian J.*, 2016, **11**, 3575-3582.
40 L. Zhou, Q. Lin, S. Liu, Y. Tan and H. Sun, *Sens. Actuators B Chem.*, 2017, **244**, 958-964.
41 R. Ren, H.-C. Xu, H. Dong, H.-T. Peng, P.-P. Wu, Y. Qiu, S.-G. Yang, Q. Sun and N.-F. She, *Talanta*, 2019, **205**, 120067.
42 H. N. Kim, M. H. Lee, H. J. Kim, J. S. Kim and J. Yoon, *Chem. Soc. Rev.*, 2008, **37**, 1465-1472.
43 W. Xu, Z. Zeng, J.-H. Jiang, Y.-T. Chang and L. Yuan, *Angew. Chem. Int. Ed.*, 2016, **55**, 13658-13699.
44 H. Chen, B. Dong, Y. Tang and W. Lin, *Acc. Chem. Res.*, 2017, **50**, 1410-1422.
45 M. Grzybowski, M. Taki, K. Senda, Y. Sato, T. Ariyoshi, Y. Okada, R. Kawakami, T. Imamura and S. Yamaguchi, *Angew. Chem. Int. Ed.*, 2018, **57**, 10137-10141.
46 X. Jiao, Y. Li, J. Niu, X. Xie, X. Wang and B. Tang, *Anal. Chem.*, 2018, **90**, 533-555.
47 L. Yuan, W. Lin, Y. Yang and H. Chen, *J. Am. Chem. Soc.*, 2012, **134**, 1200-1211.
48 R. Krishnan, J. S. Binkley, R. Seeger and J. A. Pople, *J. Chem. Phys.*, 1980, **72**, 650-654.
49 A. D. Becke, *J. Chem. Phys*, 1993, **98**, 5648-5652.
50 S. Fantacci, F. De Angelis and A. Selloni, *J. Am. Chem. Soc.*, 2003, **125**, 4381-4387.
51 M. J. Frisch, G. W. Trucks, H. B. Schlegel, G. E. Scuseria, M. A. Robb, J. R. Cheeseman, *et al*. Gaussian 09, revision D. 01. Wallingford CT: Gaussian, Inc.; 2009.

View Article Online
DOI: 10.1039/D0NJ03370G

TOC

A novel near-infrared xanthene-based fluorescent probe for detection of thiophenol in living cells and mice.